

## MULTI-WAVELENGTH OBSERVATIONS OF X-RAY SELECTED AGN: WHAT WE NEED AND WHY

M. Polletta<sup>1,2</sup> and D. M. Alexander<sup>3</sup>

<sup>1</sup>INAF - IASF Milan, via E. Bassini 15, 20133 Milan, Italy

<sup>2</sup>Institut d'Astrophysique de Paris, 98bis blvd Arago, 75014 Paris, France

<sup>3</sup>Department of Physics, University of Durham, South Road, Durham, DH1 3LE, UK

### ABSTRACT

We study the spectral energy distributions of X-ray selected AGNs to estimate the depth and sampling of optical and infrared observations necessary to detect them, and to derive accurate photometric redshifts and provide reliable spectral classifications. An overview of fields with existing or upcoming multi-wavelength coverage that satisfies those requirements is presented.

### 1. INTRODUCTION

AGN are amongst the most powerful sources and main contributors to the energy budget of the universe. They play a major role in the re-ionization of the universe (see e.g. Sokasian et al. 2003), in limiting the cooling in clusters (Balogh et al. 2001), and in regulating star formation activity in galaxies (Di Matteo et al. 2005). For these reasons, in the past decade, several multi-wavelength surveys have been carried out with a wide range of sensitivities and areas, sliding different epochs in the history of the universe with the goal to trace AGN evolution, to investigate their interplay with the environment and to understand their nature. Although significant progress has been made on various questions, a certain number of results remain uncertain and raise further questions. Below, we summarize some of the main still unanswered questions on AGNs that could be addressed by a dedicated large XMM-Newton program.

### 2. OPEN QUESTIONS ON AGNS

#### 2.1. The nature of obscuration in AGNs

Unification models (Antonucci 1993) are well established for AGNs of moderate luminosity ( $\sim 10^{43}$  ergs s<sup>-1</sup>; Seyfert galaxies). However, recent multi-wavelength studies on large AGN samples have revealed puzzling results regarding the standard AGN unification models (Antonucci 1993; Urry & Padovani 1995), especially at high luminosities. A dependency of absorption on luminosity has been discovered (Simpson 2005; Hasinger

2004), whose origin is not yet clear (Akylas & Georgantopoulos 2008). Moreover, there is emerging evidence for a mismatch between the absorption measured at various wavelengths for a significant fraction of sources (Perola et al. 2004; Tozzi et al. 2006; Sturm et al. 2006; Tajer et al. 2007; Brand et al. 2007; Polletta et al. 2008), contrarily to what is predicted by AGN unification models (Antonucci 1993). Interestingly, follow-up multi-wavelength studies of some of these obscured AGNs at high luminosities (Brand et al. 2007; Polletta et al. 2008; Sajina et al. 2007; Martínez-Sansigre et al. 2006; Ogle et al. 2006) indicate that a sizable fraction of them show properties typical of type 1 AGNs, suggesting that they are not obscured by the torus, but by cold dust at further distance.

These results raise questions on the dependency of the absorber covering factor on the AGN luminosity, on the true fraction of obscured AGNs at high luminosity and redshifts, and whether the absorber is related to the properties of the host galaxy and to the environment. In order to address these questions multi-wavelength data to trace dust and gas absorption, and AGN samples covering a complete range of absorption, luminosity and redshift are necessary.

#### 2.2. AGN dependency on the environment

An investigation that can solve several key questions regarding the AGN phenomenon, but would require a new observational program, is the study of the dependency of AGN properties on the environment. Observations indicate that the cluster galaxy population strongly evolves with redshift, e.g. both the fraction of blue, star-forming, late-type galaxies (e.g. Dressler et al. 1997; van Dokkum & Franx 2001), and X-ray and radio source over-densities increase (Best et al. 2003; Cappelluti et al. 2005; Geach et al. 2006; Eastman et al. 2007). These results imply significantly increased star-forming, starburst, and AGN activity in the past and raise the question on the physical mechanisms associated with the cluster environment that are responsible for the suppression of star formation and AGN activity and the transformation from blue to red galaxies. The processes responsible for this transformation are likely associated with the infall regions and low-density environments far from the cluster cores, and thus

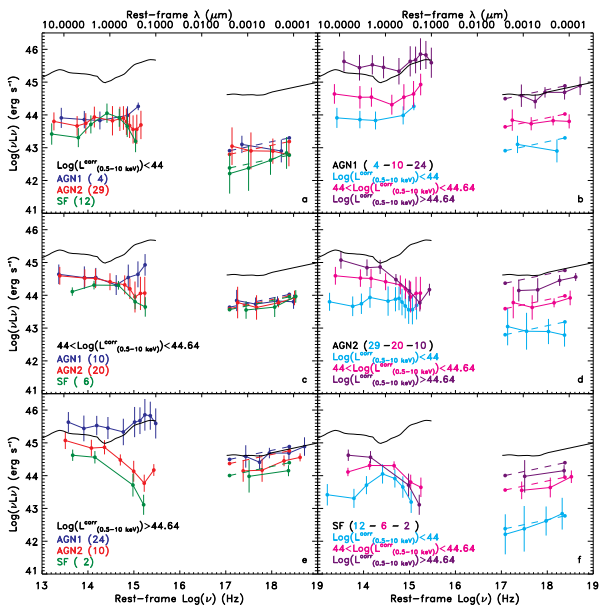


Figure 1. Left panels: Average rest-frame mid-IR-X-ray SEDs in  $\text{Log}(\nu L_\nu)$  vs  $\text{Log}(\nu)$  of all AGNs with absorption-corrected broad-band X-ray luminosity lower than  $10^{44}$   $\text{ergs s}^{-1}$  (panel a),  $10^{44} - 10^{44.64}$   $\text{ergs s}^{-1}$  (panel c), and  $>10^{44.64}$   $\text{ergs s}^{-1}$  (panel e) are shown as filled circles connected by solid lines. Uncertainties correspond to the mean absolute deviation. The X-ray SEDs are not corrected for absorption. The average SEDs for AGNs classified as star-forming galaxies (SFGs) is shown in green, for AGN2s in red and for AGN1s in blue. The dashed lines represent the average absorption-corrected 0.5–10 keV rest-frame X-ray luminosities for each AGN class and luminosity group. Right panels: Average rest-frame mid-IR-X-ray SEDs in  $\text{Log}(\nu L_\nu)$  vs  $\text{Log}(\nu)$  of all AGN1s (panel b), AGN2s (panel d), and SFGs (panel f) with absorption-corrected broad-band X-ray luminosity below  $10^{44}$   $\text{ergs s}^{-1}$  (cyan),  $10^{44} - 10^{44.64}$   $\text{ergs s}^{-1}$  (magenta), and  $>10^{44.64}$   $\text{ergs s}^{-1}$  (purple). The number of sources used to derive the average SEDs is annotated. The black solid curve represents the median template for optically-selected QSOs (Elvis et al. 1994).

require studies of the AGN population in both over-dense and under-dense regions.

The study of AGN activity as a function of a full range of environments is necessary to understand what drives the development of large-scale structures, what mechanisms facilitate SMBH fueling and growth, and what role AGNs have in the formation of galaxies. These studies are currently hampered by the difficulty of sampling a full range of environments up to high- $z$ .

In order to explore the role of environment on AGN activity it is necessary to survey a large-enough volume to probe the broadest possible range of environments (both local and large-scale structure environments), and contain enough AGNs to be able to provide statistically significant results across a range of local galaxy densities, redshifts, luminosities, AGN types (obscured/unobscured), large-scale structure environments,

and host-galaxy/SMBH mass. A wide area X-ray survey can provide enough clusters covering a broad range of masses and redshifts to be able to explore the evolution of AGN activity in galaxy clusters with large statistics and exploring new regions in the mass-redshift plane of galaxy clusters. Dense environments as galaxy clusters can be efficiently identified through X-ray observations (see e.g. Pierre et al. 2007) and AGN activity is identifiable in the hard X-ray bands even in regions of extended soft X-ray cluster emission.

### 2.3. The link between AGN activity and star formation

Several observational results provide evidence for a link between black hole (BH) growth and star formation (e.g. Gebhardt et al. 2000; Ferrarese 2002). Recent models predict coeval intense star formation and obscured AGN activity in the progenitors of massive elliptical galaxies, and that BH growth occurs in these composite systems (see e.g. Alexander et al. 2005b; Hopkins et al. 2005). The study of these systems can thus provide insights on the BH growing process, and on the origin of the relationship between bulge and BH mass (e.g. Marconi & Hunt 2003). However, observational constraints and tests to these scenarios are still lacking, mainly due to the difficulty of identifying and quantifying AGN activity in systems characterized by intense star formation (see e.g. NGC 6240, NGC 4945, and submillimeter detected AGNs Vignati et al. 1999; Alexander et al. 2005a). In most of the cases, the AGN nature of these active star-forming galaxies is revealed by their X-ray emission. Indeed, X-ray selected AGN can contain  $>20\%$  of sources with spectral energy distributions (SEDs) that are indistinguishable from those of non-AGN galaxies (Franceschini et al. 2005; Polletta et al. 2007; Tajer et al. 2007), as illustrated in Fig. 2.

Since X-ray observations are the best tracers of AGN activity in composite systems, the study of such systems requires X-ray observations of large samples of composite objects, and multi-wavelength data to separate the contribution to the bolometric luminosity from the starburst and the AGN components, to constrain their accretion and star formation rate, to estimate host stellar masses, and to probe obscuration. Such a study is becoming soon possible with the advent of Herschel and SCUBA2. These new facilities will complement existing observations, e.g. from *Spitzer* to measure the thermal emission from AGN and star-formation activity. However, although these IR observations reveal the dust-reprocessed emission, they do not provide a direct measurement of the luminosity of the primary source. X-ray observations are needed to identify these composite systems.

### 2.4. AGN SED evolution

The evolution of AGNs is still uncertain, especially at high- $z$ . Because of the difficulty of identifying obscured AGNs, the evolution of AGNs is usually derived from unobscured AGN samples (Hasinger et al. 2005; Ueda et al. 2003; Hopkins et al. 2005) which represent only about 20% of the entire AGN population, and ad hoc recipes

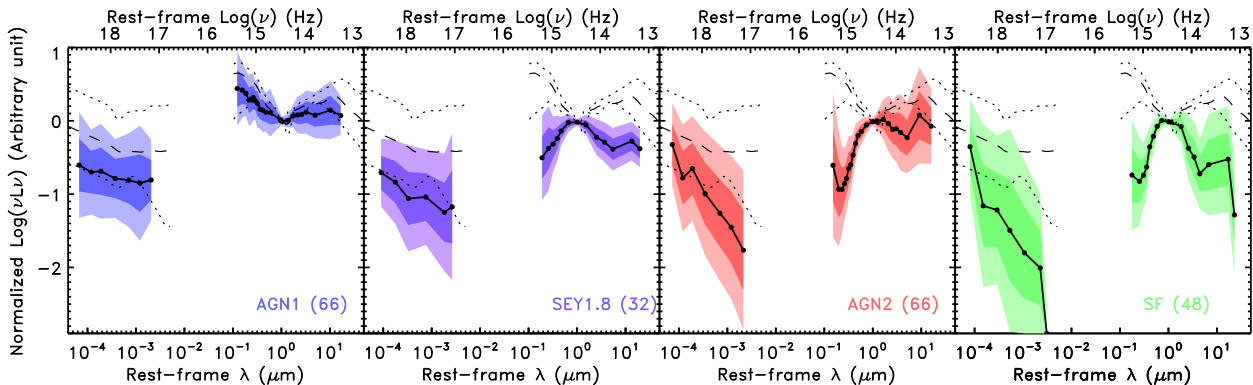


Figure 2. Normalized at  $1 \mu\text{m}$  average rest-frame X-ray–mid-IR SEDs in  $\text{Log}(\nu L\nu)$  vs  $\text{Log}(\lambda)$  (full circles connected by straight lines) of AGNs classified as AGN1 (66 sources), SEY1 (32 sources), AGN2 (66 sources) and SF (48 sources). The light and dark shaded areas correspond to  $2$  and  $1\sigma$  dispersion, respectively. Note that the X-ray luminosities are not corrected for absorption. The black thin curves represent the median (dashed curve)  $\pm 90\%$  dispersion (dotted curves) QSO template by Elvis et al. (1994).

are applied to the obscured population to reproduce the integrated observables, e.g. the X-ray background,  $z$  distributions, and the fraction of obscured AGN.

Various studies indicate a change in the AGN properties as a function of luminosity (e.g. Shemmer et al. 2006; Hasinger 2004; La Franca et al. 2005; Akylas & Georgantopoulos 2008). There are also models that predict a variation in the emitting mechanisms and thus in the observed SEDs as a function of AGN luminosity. Since the luminosity is related to the accretion rate, and thus to the fueling mechanism, and to a specific evolutionary phase, investigating what makes an AGN extremely luminous will help us to understand what triggers and fuels BH growth. To investigate what determines the AGN luminosity, we need to investigate how the AGN SEDs, their host galaxies, their environment, depend on luminosity. An example of such study is shown in Fig. 1 (adapted from Polletta et al. 2007). However, the small number of sources per luminosity bin and SED class does not allow to confirm any trend observed in the AGN SEDs as a function of luminosity.

### 3. MULTI-WAVELENGTH PROPERTIES OF X-RAY SELECTED AGNS

In order to address the questions listed above it is necessary to constrain the amount of energy produced by star-formation activity and accretion in AGNs as a function of luminosity, obscuration, black-hole and spheroid mass, host galaxy properties, and environment through cosmic times. To this end, we need large and unbiased samples of AGN covering large volumes with highly sampled multi-wavelength data. The combination of multi-wavelength data will minimize the selection effects, and provide the tools to separate the emitting energy sources, and observations of large areas will increase the statistics and provide a full range of environments.

X-ray observations are the most efficient way to select AGN samples and a selection in the hard X-ray band,

available in XMM-Newton, minimizes selection biases against absorbed AGNs. X-ray observations also provide constraints on the absorbing gas column density. The X-ray luminosity, compared with the bolometric luminosity provides the SMBH accretion rate. Optical and IR data provide a tool to classify source types, separate starburst and AGN components (e.g. Polletta et al. 2006, 2007), estimate dust absorption, characterize the host galaxy spectral type, stellar mass, and star formation activity. They can also be used to estimate photometric  $z$ , as described in § 4. Far-IR and/or sub-mm data provide a diagnostic tool to identify starburst activity as well as estimates of star-formation rates and bolometric luminosities.

### 4. ACCURACY AND RELIABILITY OF PHOTOMETRIC REDSHIFTS AND SPECTRAL CLASSIFICATION

A popular and effective technique to classify a source type (elliptical, early or late spiral, starburst, type 1 or type 2 AGN) and estimate its photometric redshifts is provided by fitting SEDs with a set of models or templates. The success of this technique depends on the quality of the photometric data, on the wavelength coverage, on the data sampling, on the model or template library, and on the type of population that is under investigation. The choice of data and templates that provide the best photometric redshifts is often not the same that provides the most reliable spectral classification. Therefore, a two step technique is sometimes required (Rowan-Robinson et al. 2005) or a compromise between the two optimal choices (Polletta et al. 2007). With a limited wavelength coverage, some photometric redshift solutions and spectral types can be degenerate, e.g., obscured starbursts and ellipticals. For example, photometric redshift estimates obtained by using only 5 SDSS bands on an X-ray sample yields 25% of outliers (Kitsionas et al. 2005). In those cases, the inclusion of mid-IR ( $>3 \mu\text{m}$  in the rest-frame) data can break the degeneracy. A comparison of

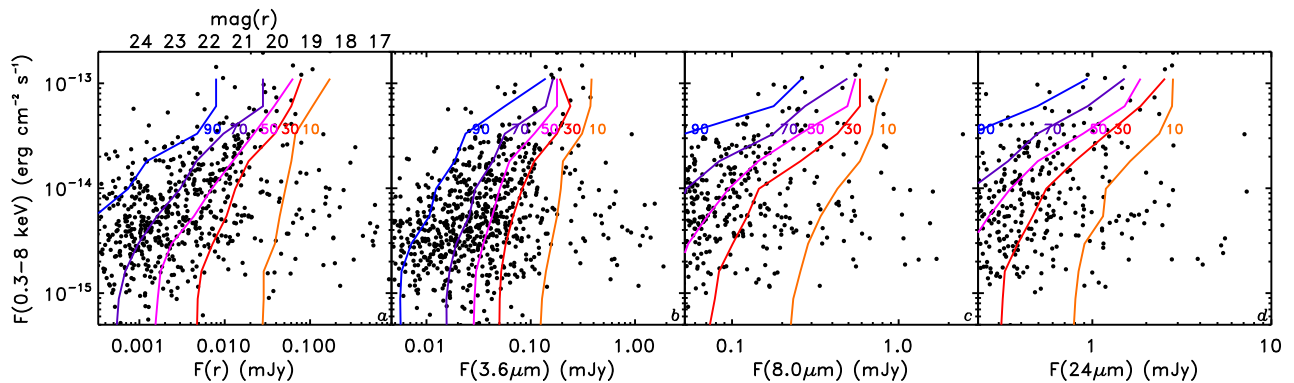


Figure 3. Broad-band ( $0.3\text{--}8\text{ keV}$ ) X-ray flux versus optical (a:  $r$ -band), and infrared (b:  $3.6\ \mu\text{m}$ , c:  $8\ \mu\text{m}$ , d:  $24\ \mu\text{m}$ ) flux for the X-ray sample in the Chandra/SWIRE survey (Polletta et al. 2006). The solid lines represent the 10% (orange), 30% (red), 50% (magenta), 70% (purple), and 90% (blue) optical or infrared detection fraction of all X-ray sources with flux above the corresponding X-ray flux limit (e.g. 90% (50%) of all X-ray sources with  $F(0.3\text{--}8\text{ keV}) > 10^{-13}\text{ ergs cm}^{-2}\text{ s}^{-1}$  have  $F(24\ \mu\text{m}) > 1$  (2) mJy).

results obtained by fitting optical+near-IR ( $\leq 4.5\ \mu\text{m}$ ) and optical+near-IR+mid-IR ( $\leq 24\ \mu\text{m}$ ) data on a hard X-ray selected sample shows that the latter method gives significantly better results both in the photometric redshift estimates and in spectral type classification (Polletta et al. 2007). The systematic mean error is  $-0.001$ , the  $rms$  is 0.12, and the outlier fraction is 10%. This accuracy is acceptable for investigating trends with luminosity, absorption and type (see e.g. Tajer et al. 2007; Polletta et al. 2007), but not to derive luminosity functions, constrain the evolution of AGNs, trace over-densities and carry out environmental studies. However, highly sampled optical-near-IR SEDs (e.g. with 14 optical-near-IR bands as in the COSMOS field) can provide photometric-redshift accuracy for X-ray sources that is comparable to that of normal galaxies (M. Salvato, priv. comm). These results open the possibility of investigating environmental dependencies with photometric redshifts.

## 5. STRATEGY AND FIELD CHOICE FOR FUTURE XMM-NEWTON SURVEYS

**1. Multiple wide fields:** In order to investigate the influence of AGNs on the environment and viceversa, it is necessary to map wide-area fields where a complete distribution of environments (superclusters, clusters, filaments, etc...) can be sampled. Moreover, multiple large-area fields reduce the impact of cosmic variance than a single very large contiguous field (Oliver et al. 2000).

**2. Good XMM-Newton visibility:** Another important factor to take into account on the field choice is good visibility to XMM-Newton and low Galactic column densities. Most of the wide ( $>4\text{ deg}^2$ ) fields already targeted by various facilities are visible for up to 10–20 ks windows, i.e. EFLS, NDWFS, ELAIS-N1, ELAIS-N2, EGS/CFHTLS-W3. A few are visible for up to 120–130 ks, i.e. XMM-LSS/CFHTLS-W1, ELAIS-S1, CDFS, CFHTLS-W2, and VVDS-D4/UKIDSS-DXS/CFHTLS-W4, and the Lockman Hole field is visible for 60 ks.

**2. Sample size:** A large AGN sample is needed to explore a broad range of parameter space and search for trends. For example, assuming 10 galaxy density bins, 5 redshift bins, 5 X-ray luminosity bins, 2 large-scale structure bins (clusters versus non-clusters), and needing 10–20 objects per bin to provide basic statistical constraints, requires a sample of up-to 10,000 AGNs. On the basis of source counts derived from deep XMM-Newton observations (e.g. Brunner et al. 2007), we estimate that this will be achieved by reaching a hard (2–10 keV) X-ray flux limit of  $3 \times 10^{-15}\text{ ergs cm}^{-2}\text{ s}^{-1}$  on a  $10\text{ deg}^2$  field or of  $10^{-14}\text{ ergs cm}^{-2}\text{ s}^{-1}$  on a  $30\text{ deg}^2$  field.

**4. Multi-wavelength coverage:** The choice of fields also depends on the existence of multi-wavelength data, in particular at optical and IR wavelengths. This requirement restricts our choice of fields to those targeted by wide multi-band optical and IR (i.e. in the near-IR and with *Spitzer*) surveys, as SWIRE, and CFHTLS.

In Fig. 3, we show the detection rates in the optical ( $r$ -band) and in 3 *Spitzer* bands as a function of broad-band X-ray flux. The data used for these estimates are from the Chandra/SWIRE survey (Polletta et al. 2006), and represent the flux range sampled by typical SWIRE (Lonsdale et al. 2003) observations. In a shallow ( $F_X > 10^{-13}\text{ ergs cm}^{-2}\text{ s}^{-1}$ ) X-ray survey, all X-ray sources will be detected in all  $r\text{--}24\ \mu\text{m}$  bands to the SWIRE limits, and 90% of X-ray sources with  $F_X \geq 3 \times 10^{-14}\text{ ergs cm}^{-2}\text{ s}^{-1}$ . In a 10 times deeper X-ray survey ( $F_X \geq 3 \times 10^{-15}\text{ ergs cm}^{-2}\text{ s}^{-1}$ ), all X-ray sources will be detected at  $3.6\ \mu\text{m}$ , 80% in the optical to  $\text{mag}(r)=25$ , 50% at  $8.0\ \mu\text{m}$ , and at  $24\ \mu\text{m}$ . Thus, an X-ray survey of  $3 \times 10^{-15}\text{ ergs cm}^{-2}\text{ s}^{-1}$  matches well the SWIRE depth. This depth can be reached by XMM-Newton with 50 ks exposures. Such a flux limit is also well suited to detect AGNs dominating the redshift peaks ( $L_X \geq 10^{43}\text{ ergs s}^{-1}$  at  $z=1.0$ , and  $L_X \geq 10^{44}\text{ ergs s}^{-1}$  at  $z=2.5$ ).

Taking into account all these requirements, the best strategy for a program that can address the questions presented in § 2 is a XMM-Newton survey of moderate depth

( $\sim 50$  ks or  $F_X \geq 3 \times 10^{-15}$  ergs cm $^{-2}$  s $^{-1}$ ) on  $\geq 3$  wide ( $> 4$  deg $^2$ ) fields with good ( $\geq 50$  ks) XMM-Newton visibility and with extensive multi-wavelength coverage. The fields that satisfy these requirements are CDFS, XMM-LSS/CFHTLS-W1, the Lockman Hole, ELAIS-S1, and CFHTLS-W4/UKIDSS-DXS.

All of these fields have been the subject of intensive multi-band deep optical imaging and over the next year PanSTARRS will start to provide deep optical coverage in 5 bands in all of them. Follow-up observations have been on-going in these fields over the last few years and are already providing a rich resource for spectroscopic redshift studies. *Spitzer* observation in all 7 bands (3.6–160  $\mu$ m) to at least the SWIRE depth are available in most of these fields. All of them will be also observed at far-IR and millimeter wavelengths by Herschel, SCUBA2 or APEX. They have (or will have) sensitive near-IR coverage from either UKIDSS (JK) or the VISTA-VIDEO surveys (zY JHK). Partial sensitive radio coverage exists in all fields, and ALMA, the EVLA, GRMT (LOFAR in future) will increase the coverage in the near future. Some of these fields already benefit from existing X-ray observations, but they are either too shallow (10–20 ks) or do not cover a wide enough contiguous area ( $< 0.6$  deg $^2$ ). The good visibility of these fields from premier observatories in both hemispheres and their range in RAs will facilitate follow-up observations.

## 6. CONCLUSIONS

We present an XMM-Newton program that could solve some key and still open questions regarding the AGN phenomenon, their role in shaping the universe, and their evolution. The program requires X-ray observations of large ( $> 10,000$  sources) AGN samples, selected in the least biased way (hard X-rays), covering a complete range of environments (superclusters, clusters, filaments, etc...), distributed on multiple fields ( $\geq 3$ ) to reduce the impact of cosmic variance, and deep enough to detect AGNs up to  $z=1.0$  ( $z=2.5$ ) with  $L_X \geq 10^{43}$  ( $10^{44}$ ) ergs s $^{-1}$ . We also require rich data sets to build SEDs, derive accurate photometric redshifts and luminosities, separate the contributions from non-AGN energy sources (host-galaxy, starburst), and estimate the amount of absorption as a function of AGN type, luminosity, redshift, and environment. A search for the best fields for this kind of program narrows down our choice to 5 fields: CDFS, XMM-LSS/CFHTLS-W1, the Lockman Hole, ELAIS-S1, and CFHTLS-W4/UKIDSS-DXS.

MP thanks Marguerite Pierre for the invitation to attend the workshop and for her patience with the delayed registration and contribution. MP acknowledges financial support from the Marie-Curie Fellowship grant MEIF-CT-2007-042111.

## REFERENCES

Akylas, A. & Georgantopoulos, I. 2008, A&A, 801, accepted [arXiv:0801.4492]

Alexander, D. M. et al. 2005a, ApJ, 632, 736  
 Alexander, D. M. et al. 2005b, Nature, 434, 738  
 Antonucci, R. 1993, ARA&A, 31, 473  
 Balogh, M. L., et al. 2001, MNRAS, 326, 1228  
 Best, P. N., et al. 2003, MNRAS, 343, 1  
 Brand, K. et al. 2007, ApJ, 663, 204  
 Brunner, H., et al. 2007, A&A, 711, accepted [arXiv:0711.4822]  
 Cappelluti, N., et al. 2005, A&A, 430, 39  
 Di Matteo, T., Springel, V., & Hernquist, L. 2005, Nature, 433, 604  
 Dressler, A., et al. 1997, ApJ, 490, 577  
 Eastman, J., et al. 2007, ApJ, 664, L9  
 Elvis, M., et al. 1994, ApJS, 95, 1  
 Ferrarese, L. 2002, ApJ, 578, 90  
 Franceschini, A., et al. 2005, AJ, 129, 2074  
 Geach, J. E., et al. 2006, ApJ, 649, 661  
 Gebhardt, K., et al. 2000, ApJ, 539, L13  
 Hasinger, G. 2004, Nuclear Physics B Proceedings Supplements, 132, 86  
 Hasinger, G., Miyaji, T., & Schmidt, M. 2005, A&A, 441, 417  
 Hopkins, P. F., et al. 2005, ApJ, 630, 705  
 Kitsionas, S., et al. 2005, A&A, 434, 475  
 La Franca, F., et al. 2005, ApJ, 635, 864  
 Lonsdale, C. J., et al. 2003, PASP, 115, 897  
 Marconi, A. & Hunt, L. K. 2003, ApJ, 589, L21  
 Martínez-Sansigre, A., et al. 2006, MNRAS, 370, 1479  
 Ogle, P., Whysong, D., & Antonucci, R. 2006, ApJ, 647, 161  
 Oliver, S., et al. 2000, MNRAS, 316, 749  
 Perola, G. C., et al. 2004, A&A, 421, 491  
 Pierre, M., et al. 2007, MNRAS, 382, 279  
 Polletta, M., et al. 2007, ApJ, 663, 81  
 Polletta, M., et al. 2008, ApJ, 673, in press [arXiv:0709.5548]  
 Polletta, M., et al. 2006, ApJ, 642, 673  
 Rowan-Robinson, M., et al. 2005, AJ, 129, 1183  
 Sajina, A., et al. 2007, ApJ, 667, L17  
 Shemmer, O., et al. 2006, ApJ, 646, L29  
 Simpson, C. 2005, MNRAS, 360, 565  
 Sokasian, A., Abel, T., & Hernquist, L. 2003, MNRAS, 340, 473  
 Sturm, E., et al. 2006, ApJ, 642, 81  
 Tajer, M., et al. 2007, A&A, 467, 73  
 Tozzi, P., et al. 2006, A&A, 451, 457  
 Ueda, Y., et al. 2003, ApJ, 598, 886  
 Urry, C. M. & Padovani, P. 1995, PASP, 107, 803  
 van Dokkum, P. G. & Franx, M. 2001, ApJ, 553, 90  
 Vignati, P., et al. 1999, A&A, 349, L57